
Article:

Li, Q., Wei, W., Li, Y. et al. (5 more authors) (2022) Development and investigation of form-stable quaternary nitrate salt based composite phase change material with extremely low melting temperature and large temperature range for low-mid thermal energy storage. Energy Reports, 8. pp. 1528-1537. ISSN 2352-4847

https://doi.org/10.1016/j.egyr.2021.12.054

Energy Reports 8 (2022) 1528–1537

Contents lists available at ScienceDirect

Energy Reports

journal homepage: www.elsevier.com/locate/egyr

Development and investigation of form-stable quaternary nitrate salt based composite phase change material with extremely low melting temperature and large temperature range for low-mid thermal energy storage

Qi Li [a], Wenzhen Wei [a], Yuying Li [a], Chuan Li [b,*], Ruihuan Ge [c], Yanping Du [d], Xinjing Zhang [e,*], Yuting Wu [a]

[a] MOE Key Laboratory of Enhanced Heat Transfer and Energy Conservation, Beijing Key Laboratory of Heat Transfer and Energy Conversion, Beijing University of Technology, Beijing, 100124, China
[b] School of Chemistry and Chemical Engineering, Shandong University of Technology, Zibo 255049, China
[c] Department of Chemical and Biological Engineering, The University of Sheffield, Sheffield S10 2TN, UK
[d] China–UK Low Carbon College, Shanghai Jiao Tong University, Shanghai 200240, China
[e] Institute of Engineering Thermophysics, Chinese Academy of Sciences, Beijing, 100190, China

ARTICLE INFO

Article history:
Received 4 October 2021
Received in revised form 1 December 2021
Accepted 15 December 2021
Available online xxxx

Keywords:
Quaternary nitrate
Form-stable composite PCM
Low melting point
Large temperature range
Thermal energy storage

ABSTRACT

This paper reports a form-stable molten salt based composite phase change material (CPCM) owning extremely low melting point and large temperature range that can be a promising candidate used in low and middle temperature thermal energy storage fields. The composite was prepared by a so-called cold compress and hot sintering approach with a eutectic quaternary nitrate of $Ca(NO_3)_2$-KNO_3-$NaNO_3$-$NaNO_2$ used as phase change material (PCM), a MgO as structure supporting material (SSM) and graphite as thermal conductivity enhancer (TCE). A series of characterizations were carried out to investigate the composite microstructure, chemical compatibility and thermal properties as well as cycling stability. The results show no chemical reaction occurred among the compositions of salt, SSM and TCEM before and after sintering, indicating excellent chemical and physical compatibility in the composite. A fairly low melting point around 89.56 °C and relatively high decomposition temperature of 628 °C were observed, giving the composite a large energy storage density over 626 kJ/kg at temperature range of 50–600 °C. A mass loading of 50% MgO gives the optimal formulation of the composite at which over 10% graphite can be involved and a thermal conductivity over 1.4 W/m· °C can be obtained. The present results indicate that such a salt based composite with fairly low melting temperature and large temperature range could be an effective alternative to organic based PCMs used in low-mid temperature thermal energy storage.

Contents

---

* Corresponding authors.
E-mail addresses: lichuan0315@hotmail.com (C. Li), Zhangxinjing@iet.cn (X. Zhang).

https://doi.org/10.1016/j.egyr.2021.12.054

1. Introduction

Worldwide energy consumption has led to an energy crisis and severe climate change (Anon, 2019a,b,c). More than 120 countries around the world have proposed carbon neutrality, aiming to build a new power system with new energy as the main body and improve energy efficiency (Christoph et al., 2019; Maryam et al., 2019). It has been broadly approved that the decarbonization of current energy system for such objectives cannot be achieved without large-scale utilization of renewable energy sources such as wind, solar and tidal energy. However, the intermittency and fluctuation characterizations of such energy sources lead to energy mismatching between supply and demand (Christoph et al., 2019; Jesus et al., 2017; Maryam et al., 2019). Energy storage presents one of the solutions towards these issues. As one of cost-effective and feasible energy storage technologies, thermal energy storage (TES) has offered great ability in resolving above challenges and also the potentials in the applications of other fields for example peak modulation of energy networks, space heating with domestic storage heaters and waste heat recovery (Kun et al., 2018; Mohamed Hany et al., 2018; Raza et al., 2019).

According to the difference of storage medium, TES technologies can be divided into three main groups of sensible heat storage, latent heat storage, and thermochemical heat storage. In particular, the latent heat storage using solid–liquid phase change materials (PCMs) has gained tremendous attentions in recent years because of the merits of isothermal melting/solidification processes, favourable energy storage density, and rational capital investment (Chuan et al., 2019c; Feng et al., 2020). A great deal of solid–liquid PCMs including organics, inorganics and eutectics have been reported and proposed at both the academic and industrial communities, in which the most appropriate candidates that suitable for low temperature (typical below 150 °C) thermal energy storage applications are organics. To overcome the conventional challenges of low thermal conductivity and liquid phase leakage of these organic materials, a so-called shape-stabilized composite phase change material (CPCM) has been recently developed and proposed. Such a CPCM is usually made of a PCM for energy storage, a skeleton structure material (SSM) for shape stabilization and a thermal conductivity enhancer (TCE) for heat transfer enhancement (the TCE can be the same as the SSM in same cases), and has been presented to achieve an excellent combination of thermophysical and mechanical properties. Cheng et al. (Wen-long et al., 2010) fabricated a paraffin/HDPE composite with the dispersion of carbon additives for low temperature TES application. It was found that the composite had a melting point of 51.2 °C and the addition of graphite can largely enhance the composite thermal conductivity. Ehid et al. (Ryan et al., 2012) investigated the use of HDPE to prevent graphite nano-particles settling within the paraffin composite. Their results revealed that a loading as little as 10 wt% HDPE can effectively eliminate the graphite materials migration inside the composite. Juarez et al. (Juarez et al., 2011) studied the performance improvement of a SEBS by mixing a paraffin based microcapsule and their results showed that a good combination of resistant and ductile performance of the SEBS based composite can be achieved with the dispersion of 1–5 wt% microcapsules. Chen et al. (Peng et al., 2016) prepared a paraffin/SEBS/HDPE composite embedded with a metal foam to address the PCM challenges of leakage and low thermal conductivity. It was found that a good chemical compatibility was achieved among the metal form, PCM, and structure supporting materials. The paraffin can be uniformly dispersed into the HDPE and SEBS, and less than 2.5 wt% mass loss of paraffin was observed after the composite experienced 50 heating and cooling thermal cycles.

It can be seen from the above literature reviews that the polymers are commonly employed as SSM for the fabrication of organic based CPCM, such composition could be able to achieve a stable structure in the composite because of the network structure formed over preparation process. However, limited by the inherent issue of low decomposition temperature, the utilization temperature for such organic-polymer composites is extremely restricted, which should typically be below 250 °C. This significantly confines the large-scale use of these materials particularly for the cases where the temperature is above 250 °C. Therefore, seeking for other promising alternatives that with relative low melting temperature and large temperature range is urgent in low temperature thermal energy storage application fields.

Inorganic salts could be one of solutions towards to this challenge because a salt mixture can be able to achieve a desired melting point through adjusting the ratio of its ingredients appropriately for which can be propitious to a broad application temperature range (Feng et al., 2020; Qi et al., 2019b). Liu et al. (Junwan et al., 2017) explored to prepare a $MgCl_2$-KCl based composite with the expanded graphite as SSM through cold compression approach, and found the uniform distribution of salt into the expanded graphite with a maximum mass loading of 85% after sintered. Later, the same authors (Junwan et al., 2018) extended their investigations by adding graphite into $MgCl_2$-KCl/expanded graphite composite to enhance the thermal conductivity with the same fabrication approach. It was revealed that the addition of graphite paper resulted in an apparent increase in composite thermal conductivity, but a decrease in enthalpy when the mass ratio of graphite paper and expanded graphite in the composite was higher than 0.88. Qin et al. (Qin et al., 2014; Yue et al., 2015) prepared and investigated a sodium sulphate–diatomite composite, and they found that the composite consisting of 45 wt% diatomite achieved the best combination of energy density and mechanical strength, in which the composite can be used at temperature as high as 980 °C. Ye et al. (Feng et al., 2014) investigated a sodium carbonate–MgO composite with multi-walled carbon nanotubes (MWCNTs) added for thermal conductivity enhancement. It is revealed that composite containing MWCNTs showed good thermal stability and a mass loss less than 5% was observed over the studied temperature range of 840–890 °C. Jiang et al. (Yifeng et al., 2018, 2019b) made a comparison study on two eutectic salt of Na_2SO_4-NaCl based composites by respectively using α-alumina and mullite as SSM, and they observed that both the two composites containing 50 wt% of salts presented high thermal stability without leakage and cracking, and a mass loss of 0.5% and 0.74%, and a decrease of latent heat around 1% and 2% occurred after 20 thermal cycles. Jiang et al. (Zhu et al., 2015) fabricated a nitrate salt based composite with cold compression–hot sintering approach by using a quaternary salt of

Table 1
Investigations on salts based composite PCM with different melting temperature by cold compression and hot sintering approach.

Composite	Salt ratio (wt.%)	Composition (wt.%)	Melting point (°C)	Latent heat (kJ/kg)	Heat capacity (kJ/kg °C)	Thermal conductivity (W/m °C)	Refs.
$LiNO_3/NaNO_3/KNO_3/Ca(NO_3)_2$-Calcium Silicate	27–16–47–10 (a)	80–20	103.5	73.59	1.65	1.177	Zhu et al. (2015)
$KNO_3/LiNO_3/Ca(NO)_3$-Expanded graphite	68–18–14	90–10	113	95.61	–	9.7	Zhuo and Zhi-Gen (2016)
$Ca(NO_3)_2/NaNO_3$-Expanded graphite	30–70 (a)	93–7	216.8	89.79	1.2539	5.7	Yunxiu et al. (2018)
$K_2CO_3/Li_2CO_3/Na_2CO_3$_MgO	10–20–10 (a)	50–50	386.4	158.7	1.48	–	Lixia et al. (2019)
$MgCl_2/KCl$-Expanded graphite	31.5–68.5 (a)	85–15	424.14	161.37	–	4.922	Junwan et al. (2017)
Li_2CO_3/Na_2CO_3-MgO-Graphite	43–57	50–50–10	498.3	178.3	–	4.3	Zhiwei et al. (2014)
$Na_2SO_4/NaCl$-α-alumina	68.05–31.95 (a)	45–55	626	117.8	–	2.05	Yifeng et al. (2019b)
$Na_2SO_4/NaCl$-mullite	68.05–31.95 (a)	45–55	626	117.6	–	1.95	Yifeng et al. (2018)
NaCl/KCl-Diatomite	70–30	1–1–0.2	657	179.3	1.07	–	Guanghui et al. (2018)
Na_2CO_3/K_2CO_3-MgO-SiC	52.2–47.8	60–40–10	710	110.2	1.65	2.28	Zhu et al. (2019a)
Na_2CO_3/K_2CO_3-MgO-glass	52–48 (a)	75–25–27.2	710	58.5	–	–	Yunkun et al. (2019)
Na_2CO_3/K_2CO_3-MgO-Kaolin	52–48	55–35–10	710	52.98	–	2.69	Bao-rang et al. (2020b)
Na_2CO_3-MgO-MWCNT	–	60–40–0.5	851	–	–	1.489	Feng et al. (2014)
Na_2SO_4-Diatomite	–	65–35	887.6	101.59	1.6	–	Tingting et al. (2015)

(a), mol.%.

$LiNO_3$-$NaNO_3$-KNO_3-$Ca(NO_3)_2$ with a mole ratio of 27%-16%-47%-10% as PCM and calcium silicate as SSM. Their results showed that the composite had a melting point of 103.5 °C and was suitable for the thermal energy storage application window over 100–585.5 °C without decomposition. Li and Wu (Zhuo and Zhi-Gen, 2016) developed a ternary nitrate salt based composite with the use of expanded graphite as SSM. 68 wt% KNO_3-18 wt% $LiNO_3$-14 wt% $Ca(NO_3)_2$ was used as PCM, and different mass ratio of $CsNO_3$ was added to achieve the good thermal stabilization of the composite. It was found that $CsNO_3$ decreased the composite fusion heat by 9.3%, but did not affect the melting point of the composite (113 °C).

Table 1 summaries the recent investigations on the inorganic salt based composites. It can be seen that the research emphasis on the salt based composites has been concentrated on fabrication of materials for middle and high temperature thermal energy storage, and very rare work have been reported on the development of low melting point inorganic salt composites used for low temperature application. This forms the main motivation of this work, in which a from-stable nitrate salt based composite with extremely low melting point and large temperature range was prepared and investigated. The composite was prepared by cold compress and hot sintering approach with a eutectic quaternary nitrate of $Ca(NO_3)_2$-KNO_3-$NaNO_3$-$NaNO_2$ used as PCM, and MgO and graphite respectively as SSM and TCE. A series of characterizations were carried out to investigate the composite microstructure, chemical compatibility and thermal properties. The results indicated the achievement of low melting temperature and large temperature range as well as enhanced properties and thermal stabilization of the salt based composite that can be a promising candidate for low temperature thermal energy storage applications.

2. Materials and methods

2.1. Raw materials

The PCM used for the composite fabrication was a eutectic quaternary nitrate that made of $Ca(NO_3)_2$, KNO_3, $NaNO_3$ and $NaNO_2$. All these salts were analytic reagent with purity of 99% and purchased from Beijing Yi-Li Chemical Co., Ltd, China. A light MgO (purity > 99%) with an average particle size of 5 μm that purchased from Tianjin Bellence Biotechnology Co., Ltd, China, was used as SSM. Natural graphite powder with an average size of 5 μm was purchased from Beijing Jia shiteng Co., Ltd, China and employed as TCE. All these materials were used directly with no extra purification.

2.2. Preparation of quaternary nitrates

The eutectic quaternary nitrate was prepared by a so-called static melting method. Specially, the raw salts of $Ca(NO_3)_2$, KNO_3, $NaNO_3$ and $NaNO_2$ were first weighed and mixed according to a pre-set mass ratio in a balance. Then, the mixed salts were transported into a corundum crucible and heated in an electrical oven (OV-11, Jeio Tech, UK) from 30 °C to 450 °C at a rate of 5 °C/min. It is pointed out that the $Ca(NO_3)_2$ is placed at the top surface of the crucible to prevent the salt climbing during the heating process. After heating at 450 °C for 24 h, the crucible containing molten salts were removed from the furnace and cooled naturally to room temperature to obtain the quaternary nitrate. Finally, the quaternary nitrate salts were taken out from the crucible and ground into fine powder with size range of 3–5 μm in a high-speed universal pulverizer. The milled quaternary nitrate salts were put into a thermal chamber (OMH 750, Thermo Scientific, Germany) for keeping dry and the further experiments.

2.3. Preparation of quaternary nitrate/mgo/graphite composite modules

The main processes for fabrication of the quaternary nitrate based composite can be summarized as follows. Step 1 was to precisely weigh the three ingredients of salt, MgO and graphite with a desired mass ratio, and then thoroughly mix the powders in a milling jar (Planetary Mill Pulverisette, Fritsch, UK) at a speed of 300 rpm for 1 h to achieve the fully mixing powder. Step 2 was to shape the mixed powder into cylindrical modules. A self-designed mould with a diameter of 12.5 mm and thickness of 20 mm is used for shaping. The mixture was put into the mould

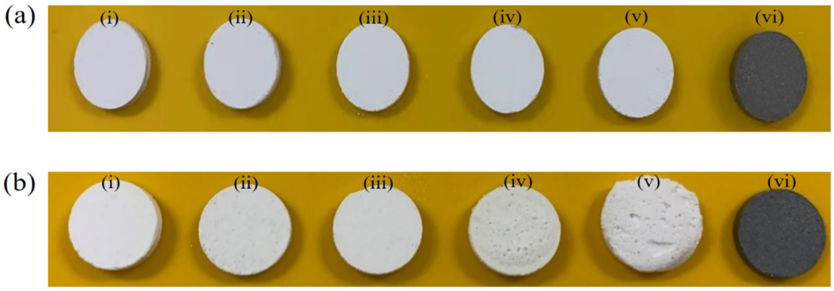

Fig. 1. Appearance of the composites before (a) and after (b) sintering: (i) S2, (ii) S3, (iii) S4, (iv) S5, (v) S6 and (vi) S5 filled with 20 wt% graphite.

Table 2
Salt based composites with different formulations and structure visual inspection after sintering.

Samples	S1	S2	S3	S4	S5	S6	S7
Salt, wt%	20	30	40	50	60	70	80
MgO, wt%	80	70	60	50	40	30	20
Graphite, wt%	∼2–20%						
Structure visual inspection (a)	■	■	■	■	○	●	●

(a): ● indicates the composite with serious structure deformation and leakage; ○ indicates the composite with little leakage and shape deformation; ■ indicates the composite has no deformation and leakage with excellent appearance.

and compressed at a uniaxial pressure of 50 MPa for 5 mins to obtain the green composite pellet. Step 3 was to sinter the composite modules. After the green pellets was prepared, they were sintered in a muffle furnace by the following temperature programme: heating at 5 °C/min from 25 °C to 150 °C, and holding at 150 °C for 1 h to remove the residual water; heating further at 5 °C/min from 150 °C to 250 °C, and holding at 250 °C for 1 h; and finally reversing the temperature programme for cooling the sample to ambient temperature.

The salt based composites got from the above steps were put into a thermal chamber for further characterizations. Through repeating the above fabrication process and adjusting the mass concentration of salt and SSM, seven composites with different formulations can be obtained and the details were tabulated in Table 2.

2.4. Characterization of the composite modules

The microstructural and morphological characteristics of the composites were observed by a Scanning Electron Microscope equipped with an energy dispersive X-ray spectroscopy detector (SEM-EDS, S4800, HITACHI, Japan). The chemical structures and stability of the composites were analysed by a Fourier transformation infrared spectroscope (FT-IR, TENSOR 27, BURKER, Germany) and an X-ray diffraction (XRD, D8, BURKER, Germany). The thermal properties of the composites including the melting temperature and latent heat were measured with a Simultaneous Thermal Analyser (STA 449F3, Netzsch, Germany). The thermal conductivity of the composites was evaluated by a Laser Flash Analyser (LFA 457, Netzsch, Germany). During measurements, each experiment was repeated at least three times to study the repeatability. The thermal cycling tests were carried out with a self-constructed and automated device comprising of a high temperature region and a low-temperature region arranged in a perpendicular manner that developed in our lab. The high temperature region could be heated to ∼1000 °C, whereas the low temperature region was maintained at 20 °C. There is a CPCM module holder linked to a linear motor via vertical shaft, enabling the motion of the sample between the hot and cold regions. A thermocouple inserted to the bottom part of CPCM sample was used to measure the sample temperature and control the thermal cycling [10. 24].

3. Results and discussions

3.1. Visual observation of composites

The appropriate loading of MgO for maintaining the structure stabilization in the composite has been checked before the microstructure characterization and chemical stability investigations are performed. For doing so, six groups of composites containing different concentrations of MgO, namely 70%, 60%, 50%, 40% and 30% that corresponding to the samples of S2–S6 listed in Table 1, are fabricated and tested. Fig. 1 shows the results that obtained from the visual observation for the composites S2–S6 before and after sintering. The results for samples S1 and S7 are not given since serious deformation or excellent appearance are apparent for these two formulations. It can be seen from the figure that there is the occurrence of obvious shape deformation and salt leakage of the composites when the MgO loading is less than 50 wt%, indicating that at least 50 wt% MgO is required to ensure the composite structure stabilization. Therefore, sample S4 is deemed as the optimal formulation and being selected for the following discussion. To further investigate the maximum graphite loading in the composite, visual inspections have also been carried out on the sample S4 containing different amount of graphite. As shown in Fig. 1 (b-vi), the composite containing 20 wt% graphite presents excellent appearance beyond which apparent deformation and leakage are occurred, demonstrating 50 wt% loading of MgO endues the composite with the capability to accommodate 20% graphite maximally.

3.2. Morphological and microstructural observations

Fig. 2(a) and (b) show SEM images of the salt based composite with a mass ratio of PCM:SSM:TCE=5:5:1 before sintering. One can see that a uniform distribution of salt, MgO and graphite in the composite after the compression process. The spherical shape of the MgO makes the salt and graphite particles occupied the interspaces and voids in the composite to form a dense structure. Fig. 2(c) and (d) show the salt based composite after sintering. One can see an apparent and significant change to the composite structure. A molten salt liquefied structure (MSLS) is obvious and the existence of such structure plays a key role in holding the particles together and keeping the structure stabilization. Our previous work (Chuan et al., 2019a; Qi et al., 2020a) has indicated the microstructure formation mechanism of such salt based composites. In a salt based composite containing ceramics as SSM, the solid–liquid transition of salt during the sintering process brings into pressure difference, leading to the liquid salt flowing into the voids and pores in the composite. Meanwhile, the wetted liquid salt pulls the high surface energy ceramics together and rearrange them. Liquid bridges between the salt and ceramic particles would generate in such a process to overcome the swelling effects of graphite, promoting rigid and densification of the composite structure.

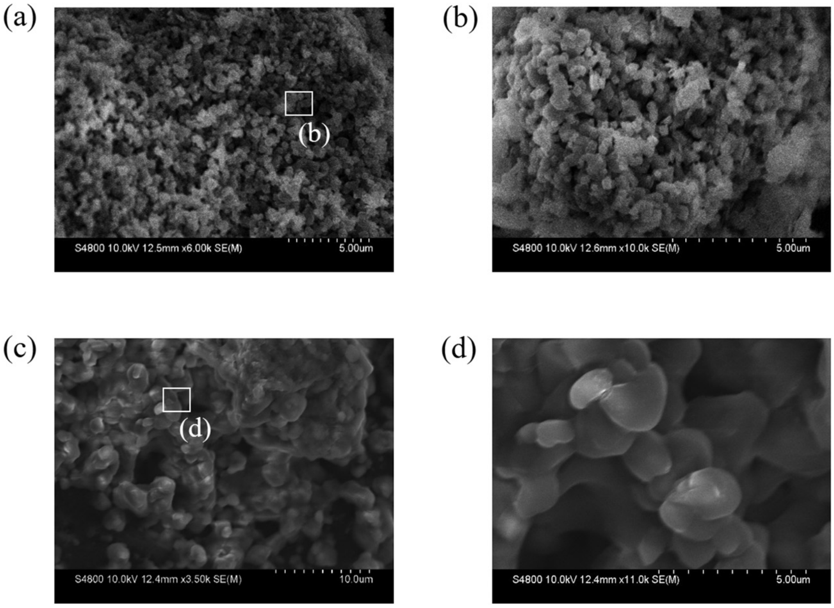

Fig. 2. (a) SEM image of the salt based composite with mass ratio of PCM:SSM:TCE=5:5:1 before sintering; (b) Capture SEM image from the rectangular area of Fig. (a); (c) SEM image of the salt based composite with mass ratio of PCM:SSM:TCE=5:5:1 after sintering; (d) Capture SEM image from the rectangular area of Fig. (c).

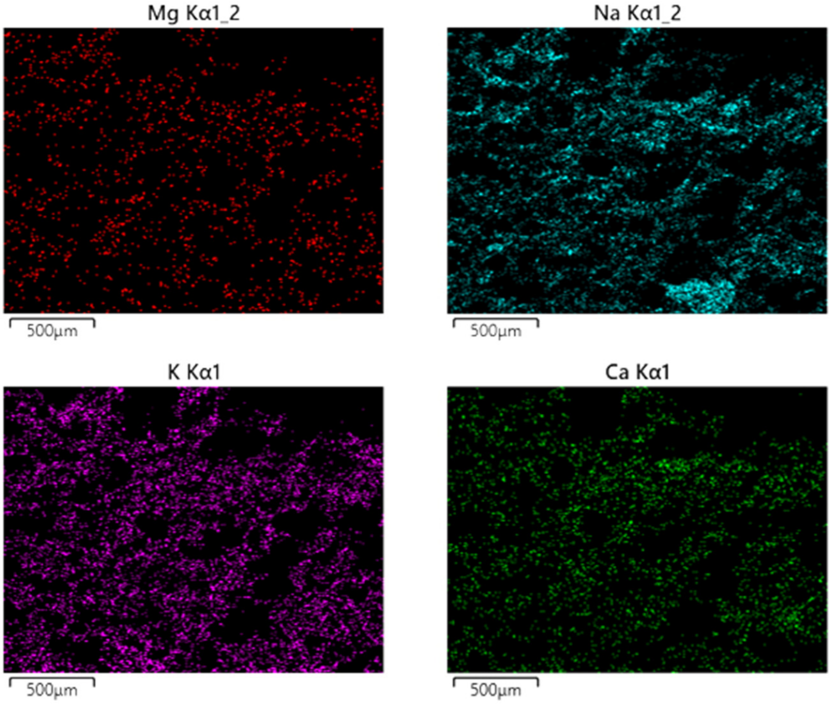

Fig. 3. EDS element mapping images of the salt based composite with mass ratio of PCM:SSM:TCE = 5:5:1.

Fig. 3 shows the element distribution diagrams of the salt based composite. It can be seen from the figure that the elements of Mg, Na, Ca and K are fully filled and occupied the whole observation region. This further indicates that the quaternary salt and the MgO skeleton are tightly combined and evenly distributed in the composite. Such an observation can be explained as follows. In the salt–MgO composite, the micro-scale movement of the liquid salt leads to the migration and rearrangement of ceramics because of the high surface energy of MgO towards the salt. Over such a process, the particles redistribution occurs, which leads to an increase in the homogeneity of the microstructure, and allows the formation of a dense and uniform composite.

3.3. Chemical compatibility among the compositions

The chemical compatibility of the quaternary nitrate, MgO, graphite and salt based composites is determined from the XRD and FT-IR analysis at a temperature of 25 °C. The XRD results are plotted in Fig. 4, and it can be seen that four main diffraction peaks at approximately $2\theta = 26.4°$, $42.8°$, $62.2°$ and $78.5°$ are observed in the salt based composite before sintering, which are similar with the quaternary nitrate, MgO and graphite, indicating the same crystal structures have achieved in the salt based composites. It can also be seen from the figure that only a single diffraction peak of 26.1° is apparent for graphite. Such

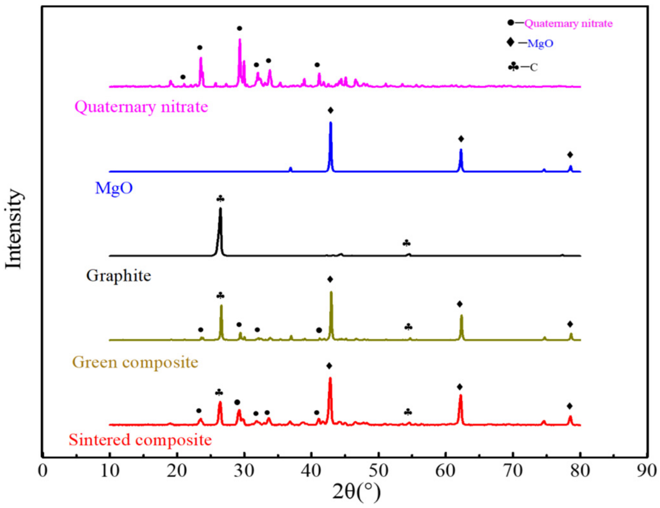

Fig. 4. XRD patterns of composites: quaternary nitrate, MgO, graphite, composite before and after sintering.

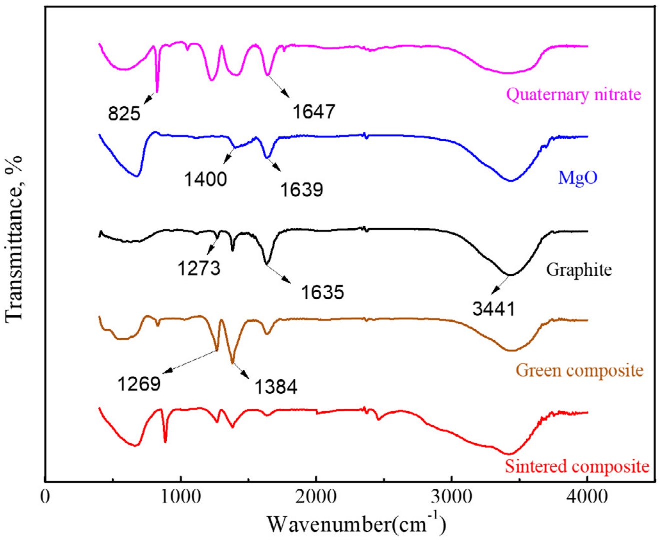

Fig. 5. FT-IR spectra of composites: quaternary nitrate, MgO, graphite, composite before and after sintering.

observation is similar to that of the nano-graphite (Yaojie et al., 2016) and expanded graphite (Lifang et al., 2019). For the salt based composite after sintering, there are also only the peaks of $2\theta = 26.4°$, 42.8°, 62.2° and 78.5° appeared, suggesting that there is no chemical reaction among the quaternary nitrate, MgO and graphite, and an excellent chemical compatibility is achieved in the composite.

The FT-IR analysis on the chemical structures of the quaternary salt, MgO, graphite and salt based composite before and after sintering is shown in Fig. 5. It can be seen that there are several absorption peaks of 825 cm^{-1}, 1269 cm^{-1}, 1384 cm^{-1}, and 1647 cm^{-1} apparent. These peaks are associated with the in-plane flexural vibration of NO_3^{-1}, stretching vibration of NO_2^{-1} and antisymmetric stretching vibration of NO_3^{-1}. For the MgO, two main peaks of 1400 cm^{-1} and 1639 cm^{-1} are observed. These peaks are mainly caused by the stretching vibration of the Mg–O bond. It is needed to notice that due to the existence of residual water, a characteristic peak of –OH stretching vibration occurring at 3441 cm^{-1} is obvious for all measured samples. For the salt based composites before and after sintering, they present the same spectrum peaks as the quaternary salt, MgO and graphite, as illustrated in Fig. 5. These observations further indicate that there is no chemical reaction occurred in the salt–MgO–graphite composite, and all the ingredients are chemically compatible.

3.4. Phase change properties of the composites

In order to efficiently and effectively evaluate the fabricated quaternary salt based composites, the thermal properties of the composites including phase change temperature and latent heat as well as specific heat capacity are tested by DSC. The results are depicted in Fig. 6 and the relevant measured data are summarized in Table 3. One can see that only one main peak is observed for all measured samples and a decrease in the mass ratio of salt in the composites yields a gradual reduction in the peaks of heat flow independently. Because of no chemical reaction among the compositions, all the composites exhibit similar melting characteristics. As shown in Table 3, a fairly low melting temperature below 100 °C is observed for all the three measured samples. The onset phase change point for the salt–MgO–Graphite composite is only around 89 °C, which is the lowest value for the inorganic salts among the open literature. This indicates the developed salt based composite can replace the organics being used in low temperature thermal energy storage fields.

Table 3 also gives the latent heat and specific heat capacity of the measured samples. One can see that the latent heat values of either the pure quaternary salt or the salt based composite are not large. It seems that the small value of latent heat would be a challenge for the utilization of the salt–MgO composite particularly for the cases of a narrow temperature range. However, for a condition where the temperature swing is large and the organics cannot be used, the developed salt–MgO composite would be an effective choice. Therefore, to comprehensively evaluate the composite energy storage ability, the total energy storage density, relating to the energy storage through both the latent and sensible forms, is used and calculated by the following equation (Qi et al., 2020a; Zhu et al., 2015):

$$Q_t = \varepsilon \int_{T_0}^{T_s} c_{p,ssm} dT + \xi \int_{T_0}^{T_s} c_{p,tce} dT + \eta \left(\int_{T_0}^{T_m} c_{ps,pcm} dT + \Delta H_m + \int_{T_m}^{T_s} c_{pl,pcm} dT \right) \quad (1)$$

where Q_t is the total storage energy in the composite at a temperature range of $T_0 - T_s$, T_0 and T_s mean the start and stop temperatures in a charging or discharging process, ε, ξ and η are respectively the mass ratios of SSM, TCE and PCM in the composite, $c_{p,ssm}$ and $c_{p,tce}$ respectively stand for the heat capacity of the SSM and TCE, $c_{ps,pcm}$ and $c_{pl,pcm}$ represent the heat capacities of the solid PCM and liquid PCM, respectively. Using the above equation together with the measured heat capacity value, one can obtain the composite total energy storage density. As summarized in Table 3, for a given temperature range of 50–600 °C, the energy storage density of the composite reaches up to 629.56 kJ/kg, which is higher than most organics and hence could be a competitive alternative used in low-mid temperature thermal energy storage areas.

3.5. Thermal conductivity of the composites

The addition of graphite has been reported to be able to effectively enhance the composite thermal conductivity. In this section, the thermal conductivities of the salt–MgO composites containing different mass loading of graphite are investigated.

Table 3
Phase transition parameters of the quaternary nitrate and composites.

Name	Onset (°C)	Peak (°C)	Endset (°C)	Specific heat (J/g °C)	Latent heat (kJ/kg)	Energy storage density (kJ/kg), 50–600 °C
Pure salt	86.14	96.7	181.92	1.407	72.53	846.38
Salt–MgO	89.09	96.1	179.25	0.95	39.89	622.39
Salt–MgO–C	89.56	96.7	180	0.967	37.71	629.56

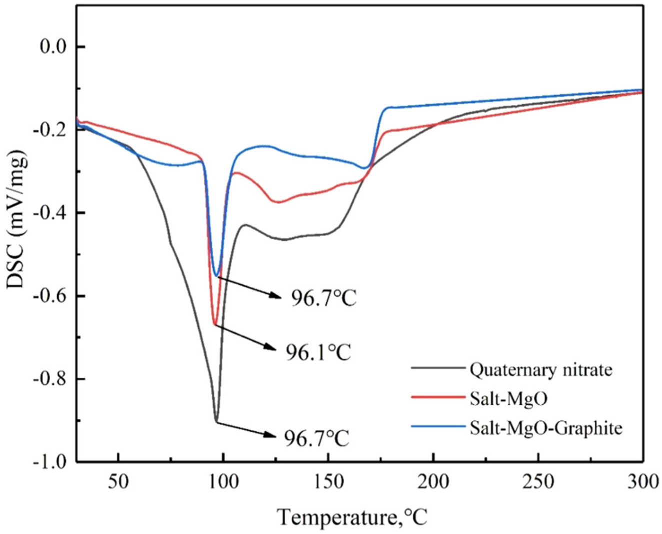

Fig. 6. DSC curves of the samples including pure quaternary nitrate, Salt–MgO composite with a mass ratio of 5:5 and Salt–MgO–Graphite composite with a mass ratio of 5:5:1.

For doing so, the composites with different mass concentration of graphite over range of 2%–20% are measured. The detailed measuring results and fitting curve are plotted in Fig. 7. One can see that, for a given measurement temperature of 50 °C, the composite thermal conductivity is increased with the increase of graphite loading. The thermal conductivity of the composite with no graphite at the measuring temperatures of 50 °C is 0.954 W/m· °C, which respectively increase to 1.41 W/m· °C and 1.605 W/m· °C when the graphite contents are 10% and 20%. Also included in Fig. 7 is the variation of the composite thermal conductivity with measured temperature. One can see that, for the composites containing 2 wt% and 10 wt% graphite, the measured value decreases with the increase of temperature, indicating the composite heat transfer ability gradually reduces with the temperature. A similar trend has also been reported by Navarro et al. (Navarro et al., 2016), who investigated the thermal conductivity of a $NaNO_3$-MgO-C composite and indicated that the thermal conductivity can be associated with the Debye temperature. Namely, the composite thermal conductivity decreases with temperature for a given measurement condition above Debye temperature. The detailed reason for such observations remains to be further explored, but the results illustrated in Fig. 7 clearly demonstrate that the composite thermal conductivity can be significantly enhanced by the addition of graphite.

The developed quaternary nitrate composite has a low melting temperature (~89 °C) that can be used in low-mid temperature fields. Therefore, it is interested to compare its thermal conductivity with that of other materials having a similar melting temperature range. Fig. 8 plots the comparison results, in which the thermal conductivity measurement values of several common PCMs with a melting point around 100 °C are involved. It can be seen that the thermal conductivity of the present salt based composite is far higher than that of $Mg(NO_3)_2 \cdot 6H_2O$ and $MgCl_2 \cdot 6H_2O$. For a fixed mass concentration of 10 wt% graphite, the composite thermal conductivity is respectively 2, 1.5, 1.2 and 1.06 times higher than that of paraffin composite, HDPE composite, salt–calcium silicate and erythritol composites. All these observations imply the developed quaternary nitrate composite in this work achieves a high thermal conductivity, and could be a promising candidate for low-mid temperature thermal energy storage applications.

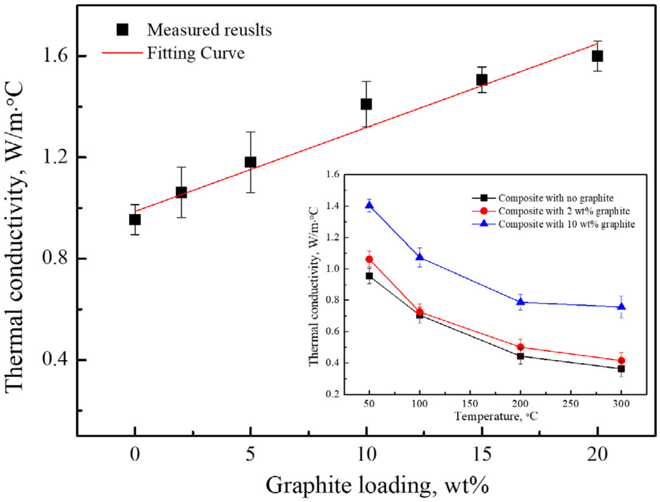

Fig. 7. Thermal conductivity of the composites containing different mass ratio of graphite.

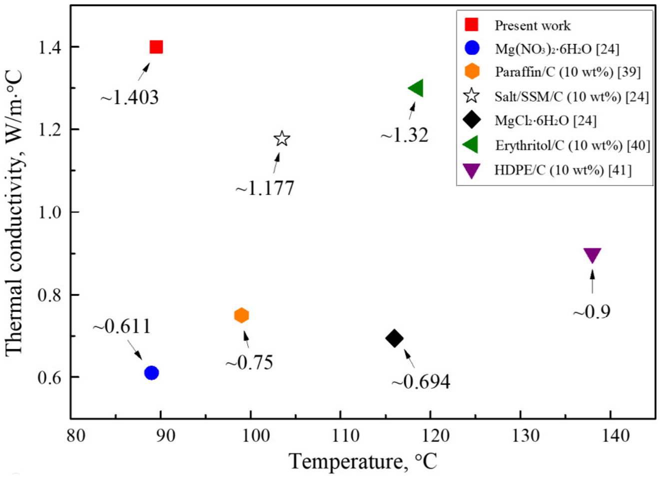

Fig. 8. Thermal conductivity comparison of several PCMs suitable for low-mid temperature thermal energy storage.

3.6. Thermal stability and cycling stability of the composites

Fig. 9 presents the thermogravimetric analyses for the quaternary nitrate and salt–MgO composite. One can see that the thermal decomposition of the quaternary nitrate is took place

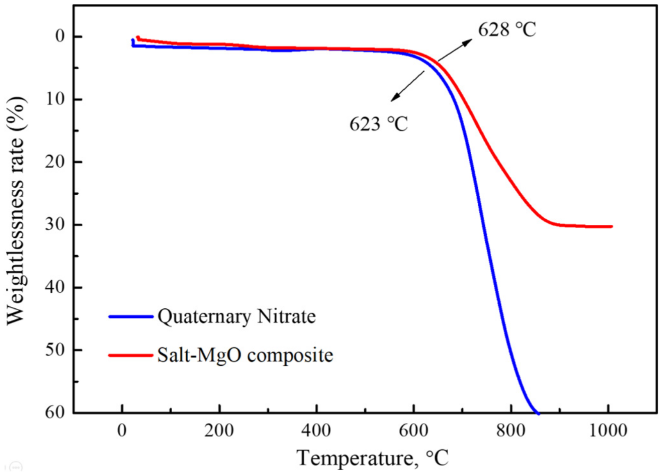

Fig. 9. TG curves of the quaternary nitrate and salt based composite.

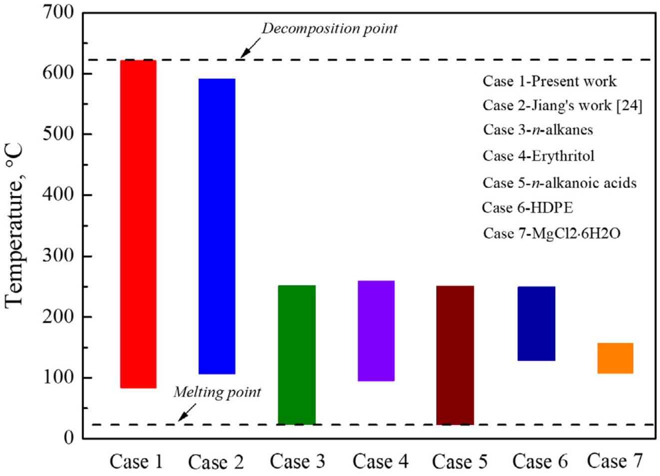

Fig. 10. Comparison of temperature range from melting point to decomposition point between present work and other typical materials.

through one-step process starting from 601 °C, which is higher than other multicomponent nitrate salts reported in the literature. When dispersing MgO into the quaternary nitrate, as shown in Fig. 9, the thermal decomposition temperature of the quaternary nitrate is enhanced. It has been reported that the thermal deposition temperature or maximum operation temperature can be referred as the temperature moment when more than 3% of the initial weight has been forfeited (Qi et al., 2020a). Therefore, the thermal decomposition temperatures for quaternary nitrate and salt based composite can be determined as 623 °C and 628 °C accordingly. The maximum operating temperature of the salt based composite is slightly higher than that of the pure salt, confirming that the molten salt liquefied structure formed over the cold compression–hot sintering process is profitable for the improvement of thermal stability of quaternary salt. An examination of the figure also finds that, for a given potential application with large temperature swing, e.g., 50–600 °C, there is no mass loss observed for the composite. Considering the composite phase transition temperature of 89 °C is far less than 600 °C, it is therefore asserted that the composite developed in this work achieves outstanding thermal stability with low melting point and large temperature range that suitable for low and middle temperature TES applications.

As mentioned above, one of the main advantages of the quaternary nitrate based composite is the high decomposition temperature that endow the composite with the wider temperature range and ability to be used in some extreme energy storage systems such as industrial waste heat recovery and peak shaving of energy networks. For comparison, the decomposition temperatures of some typical PCMs reported in the literature that suitable for low-mid temperature applications have been measured and analysed. The results are summarized in Fig. 10. One can see that the developed composite acquires the largest temperature range whereas the others only presents a narrow stable temperature range particularly for the organics and $MgCl_2·6H_2O$. Here, the temperature range refers to the difference between the decomposition temperature and melting temperature. As illustrated in Fig. 10, the temperature range of the salt–MgO composite reaches up to 539 °C, which is almost twice as high as that of the alkanes and alkanoic acids, and 10 times higher than the $MgCl_2·6H_2O$. In general, a PCM with wider temperature range means it has higher ability to take risks of decomposition when the utilization temperature is fairly higher than its melting point. This analysis, together with the results presented in Figs. 6 and 9, therefore demonstrate that the developed quaternary nitrate based composite achieves a fairly low melting point and wider temperature range that can be effective alternative to the organic PCMs used in low and middle temperature thermal energy storage fields.

Thermal cycling stability of the salt based composites are investigated by conducting the XRD and FT-IR checks on the samples before and after experienced 100 times of thermal cycles. Fig. 11 shows the results. By analysing these two figures (Fig. 11(a) and (b)), one can see that all the diffraction peaks in the two composites are the same as that in the pure materials and the composites that experienced one thermal cycle. These observations reveal that no new compound is created in the composite over the repeated heating–cooling cycles, further demonstrating that all the compositions are chemically compatible and a good chemical stability has been achieved in the composite.

Fig. 12 shows the DSC curves of the composites before and after 100 heating–cooling cycles. One can see that both the phase change temperature and latent heat of the composite before and after experienced 100 thermal cycles varies a little. The onset, peak and endset temperatures of the composites change from 89.56 °C to 90.2 °C, 96.7 °C to 97.8 °C, and 180 °C to 181.2 °C, respectively. As for the latent heat, the value varies around 4% decreasing from 37.71 kJ/kg to 36.2 kJ/kg. The reason can be attributed to the salt leakage over the repeated heating–cooling cycles. In the salt–MgO composite, because of the involvement high wettability of ceramics, most of the salt can be effectively encapsulated in the composite structure, but for the salt located at exterior surface could occur the leakage because of the defective accommodation of salt in these areas. In spite of this, all of these modifications are in an acceptable level, which do not affect the salt based composites being as ideal candidates used in thermal energy storage systems. To sum up, both the XRD, FT-IR and DSC measurement results presented in Figs. 10 and 11 indicate that the composite developed in this work achieves an outstanding thermal cycling stability that suitable for low-temperature thermal energy storage applications.

4. Conclusions

A form-stable salt based composite with a fairly low melting temperature and large temperature range that suitable for low and middle temperature thermal energy storage was prepared and investigated in this work. The composite was fabricated by a cold compress–hot sintering approach with the use of a eutectic quaternary nitrate as PCM, a MgO as SSM and graphite as TCE. The leakage inspection was first conducted to confirm the optimum

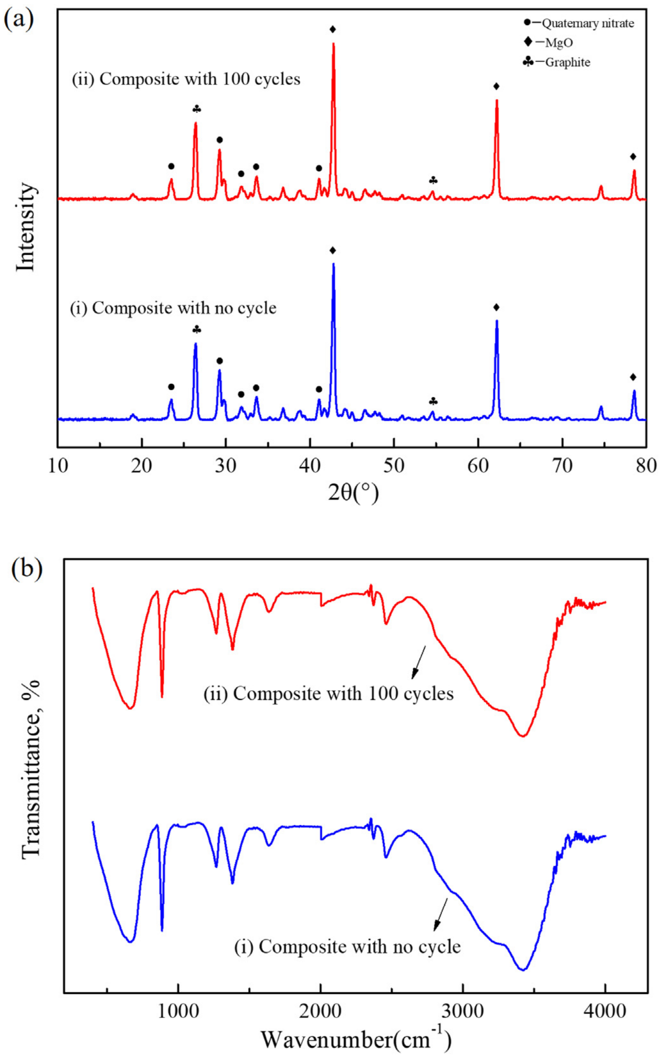

Fig. 11. Cycling stability of the composites before and after 100 times heating–cooling cycles. (a) XRD patterns and (b) FT-IR analysis.

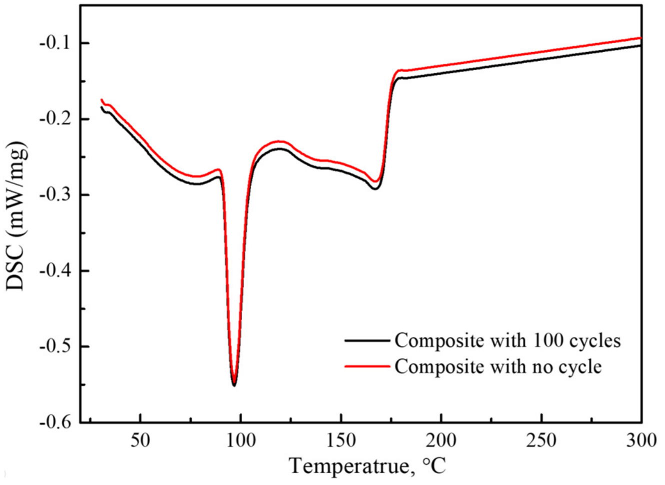

Fig. 12. DSC curves of the composites material before and after 100 times heating–cooling cycles.

composition within the composite. A series of characterizations were then performed to evaluate the composite microstructure, chemical compatibility and structure, thermal properties, and thermal conductivity. Finally, the thermal reliability and cycling stability was analysed. Based on the investigations, the following conclusions can be obtained.

(1). SEM observation demonstrates a clearly molten salt liquefied structure formed in the composite. Owning to such structure, the salt can be effectively accommodated and the leakage of liquid phase can therefore be prevented during phase transition process.

(2). The results of FT-IR and XRD characterizations indicate that there is no chemical reaction among the quaternary nitrate salt, MgO and graphite, and an excellent chemical compatibility is achieved in the composite.

(3). The DSC and TG results show that the salt–MgO–graphite composite with a mass ratio of 50:50:10 presents a fairly low melting temperature around 89 °C, high decomposition temperature over 625 °C and large energy storage density of 629.39 kJ/kg. Such a low melting temperature and large temperature range endow the composite with ability to be as promoting alternative to organic based PCMs used in low and middle thermal energy storage fields.

(4). The LFA measurement result presents that the salt–MgO–graphite composite achieves a high thermal conductivity. The measured value reaches up to 1.41 W/m· °C, which is far higher than that of $Mg(NO_3)_2\cdot 6H_2O$ and $MgCl_2\cdot 6H_2O$. For a fixed mass concentration of 10 wt% graphite and similar melting temperature range of 100 °C, the composite thermal conductivity is respectively 2, 1.5, 1.2 and 1.06 times higher than that of paraffin composite, HDPE composite, salt–calcium silicate and erythritol composites.

Declaration of competing interest

The authors declare that they have no known competing financial interests or personal relationships that could have appeared to influence the work reported in this paper.

Acknowledgements

The work was supported by the high-end talents development programme of Beijing University of Technology, China, Taishan Scholar Foundation (Grant No. tsqn201909110), and International Research Cooperation Seed Fund of Beijing University of Technology, China (Project No. 2021B40).

References

Anon, 2019a. Net Zero: The UK's Contribution to Stopping Global Warming. Committee on Climate Change.

Anon, 2019b. Net-zero by 2050: Investor risks and opportunities in the context of deep decarbonisation of electricity generation.

Anon, 2019c. Zeroing in: Capturing the opportunities from a UK net zero emission target.

Bao-rang, Li, Hui, Tan, Yu, Liu, Qi, Liu, Gao-qun, Zhang, Zhan-feng, Deng, Gui-zhi, Xu, Yong-Quan, Guo, Xiao-ze, Du, 2020b. Experimental investigations on the thermal stability of Na_2CO_3-K_2CO_3 eutectic salt/ceramic composites for high temperature energy storage. Renew. Energy 146, 2556–2565.

Christoph, Bott, Ingo, Dressel, Peter, Bayer, 2019. State-of-technology review of water-based closed seasonal thermal energy storage systems. Renew. Sustain. Energy Rev. 113, 109241.

Chuan, Li, Qi, Li, Lin, Cong, Yongliang, Li, Xianglei, Liu, Yimin, Xuan, Yulong, Ding, 2019a. Carbonate salt based composite phase change materials for medium and high temperature thermal energy storage: A microstructural study. Sol. Energy Mater. Sol. Cells 196, 25–35.

Chuan, Li, Qi, Li, Yongliang, Li, Xiaohui, She, Hui, Cao, Peikun, Zhang, Li, Wang, Yulong, Ding, 2019c. Heat transfer of composite phase change material modules containing a eutectic carbonate salt for medium and high temperature thermal energy storage applications. Appl. Energy 238, 1074–1083.

Feng, Jiang, Lingling, Zhang, Xiaohui, She, Chuan, Li, Daqiang, Cang, Xianglei, Liu, Yimin, Xuan, Yulong, Ding, 2020. Skeleton materials for shape-stabilization of high temperature salts based phase change materials: A critical review. Renew. Sustain. Energy Rev. 119, 109539.

Feng, Ye, Zhiwei, Ge, Yulong, Ding, Jun, Yang, 2014. Multi-walled carbon nanotubes added to Na_2CO_3/MgO composites for thermal energy storage. Particuology 15, 56–60.

Guanghui, Leng, Geng, Qiao, Zhu, Jiang, Guizhi, Xu, Yue, Qin, Chun, Chang, Yulong, Ding, 2018. Micro encapsulated & form-stable phase change materials for high temperature thermal energy storage. Appl. Energy 217, 212–220.

Jesus, Lizana, Ricardo, Chacartegui, Ange, Barrios-Padura, Manuel, Valverde Jose, 2017. Advances in thermal energy storage materials and their applications towards zero energy buildings: A critical review. Appl. Energy 203, 219–239.

Juarez, D., Ferrand, S., Fenollar, O., Fombuena, V., Balart, R., 2011. Improvement of thermal inertia of styrene-ethylene/butylene-styrene (SEBS) polymers by addition of microencapsulated phase change material (PCMs). Eur. Polym. J. 47, 153–161.

Junwan, Liu, Min, Xie, Ziye, Ling, Xiaoming, Fang, Zhengguo, Zhang, 2018. Novel $MgCl_2$-KCl/expanded graphite/graphite paper composite phase change blocks with high thermal conductivity and large latent heat. Sol. Energy 159, 226–233.

Junwan, Liu, Qianhao, Wang, Ziye, Ling, Xiaoming, Fang, Zhengguo, Zhang, 2017. A novel process of preparing molten salt/expanded graphite composite phase change blocks with good uniformly and small volume expansion. Sol. Energy Mater. Sol. Cells 169, 280–286.

Kun, Du, John, Calautit, Zhonghua, Wang, Yupeng, Wu, Hao, Liu, 2018. A review of the applications of phase change materials in cooling, heating and power generation in different temperature ranges. Appl. Energy 220, 242–273.

Lifang, Liu, Jiayu, Chen, Yue, Qu, Tao, Xu, Huijun, Wu, Gongsheng, Huang, Xiaoqing, Zhou, Lixiu, Yang, 2019. A foamed cement blocks with paraffin/expanded graphite composite phase change solar thermal absorption material. Sol. Energy Mater. Sol. Cells 200, 110038.

Lixia, Sang, Feng, Li, Yongwang, Xu, 2019. Form-stable ternary carbonates/MgO composite material for high temperature thermal energy storage. Sol. Energy 180, 1–7.

Maryam, Arbabzadeh, Ramteen, Sioshansi, Johnson, Jeremiah X., Keoleian, Gregory A., 2019. The role of energy storage in deep decarbonization of electricity production. Nature Commun. 10, 3413.

Mohamed Hany, Abokersh, Mohamed, Osman, Omnia, El-Baz, Mohamed, El-Morsi, Osama, Sharaf, 2018. Review of the phase change materials (PCM) usage for solar domestic water heating systems (SDWHS). Int. J. Energy Res. 42, 329–357.

Navarro, M.E., Andreu, P., Qiao, G., Ding, Y., Thermal properties of a novel medium temperature thermal energy storage composite based on sodium nitrate as phase change material. In Proceedings of the 12th International Conference on Heat Transfer, Fluid Mechanics and Thermodynamic, Costa de Sol, Spain. 2016. pp. 11-13.

Peng, Chen, Xuenong, Gao, Yaqin, Wang, Tao, Xu, Yutang, Fang, Zhengguo, Zhang, 2016. Metal foam embedded in SEBS/paraffin/HDPE form-stable PCMs for thermal energy storage. Sol. Energy Mater. Sol. Cells 149, 60–65.

Qi, Li, Chuan, Li, Zheng, Du, Feng, Jiang, Yulong, Ding, 2019b. A review of performance investigation and enhancement of shell and tube thermal energy storage device containing molten salt based phase change materials for medium and high temperature applications. Appl. Energy 255, 113806.

Qi, Li, Lin, Cong, Xusheng, Zhang, Bo, Dong, Boyang, Zou, Zheng, Du, Yaxuan, Xiong, Chuan, Li, 2020a. Fabrication and thermal properties investigation of aluminium based composite phase change material for medium and high temperature thermal energy storage. Sol. Energy Mater. Sol. Cells 211, 110511.

Qin, Y., Yu, X., Leng, G.H., Zhang, L., Ding, Y.L., 2014. Effect of diatomite content on diatomite matrix based composite phase change thermal storage material. Mater. Res. Innov. 18, S2-453-S2-456.

Raza, Gulfam, Peng, Zhang, Zhaonan, Meng, 2019. Advanced thermal systems driven by paraffin-based phase change materials-a review. Appl. Energy 238, 582–611.

Ryan, Ehid, Weinstein, Randy D., Fleischer, Amy S., 2012. The shape stabilization of paraffin phase change material to reduce graphite nanofiber settling during the phase change process. Energy Convers. Manage. 57, 60–67.

Tingting, Qian, Jinhong, Li, Xin, Min, Yong, Deng, Weimin, Guan, Lei, Ning, 2015. Diatomite: A promising natural candidate as carrier material for low, middle and high temperature phase change material. Energy Convers. Manage. 98, 34–45.

Wen-long, Cheng, Rong-ming, Zhang, Kun, Xie, Na, Liu, Jun, Wang, 2010. Heat conduction enhanced shape-stabilized paraffin/HDPE composite PCMs by graphite addition: Preparation and thermal properties. Sol. Energy Mater. Sol. Cells 94, 1636–1642.

Yaojie, Tang, Di, Su, Xiang, Huang, Guruprasad, Alva, Lingkun, Liu, Guiyin, Fang, 2016. Synthesis and thermal properties of the MA/HDPE composites with nano-additives as form-stable PCM with improved thermal conductivity. Appl. Energy 180, 116–129.

Yifeng, Jiang, Yanping, Sun, Jacob, Rhys D., Frank, Bruno, Sean, Li, 2018. Novel Na_2SO_4-NaCl-ceramic composites as high temperature phase change material for solar thermal power plants (Part I). Sol. Energy Mater. Sol. Cells 178, 74–83.

Yifeng, Jiang, Yanping, Sun, Sean, Li, 2019b. Performance of novel Na_2SO_4-NaCl-ceramic composites as high temperature phase change materials for solar power plants (Part II). Sol. Energy Mater. Sol. Cells 194, 285–294.

Yue, Qin, Guanghui, Leng, Xiang, Yu, Hui, Cao, Geng, Qiao, Yunfeng, Dai, Yelong, Zhang, Yulong, Ding, 2015. Sodium sulfate-diatomite composite materials for high temperature thermal energy storage. Powder Technol. 282, 37–42.

Yunkun, Lu, Gaoqun, Zhang, Junjie, Hao, Zhongkai, Ren, Zhanfeng, Deng, Guizhi, Xu, Cenyu, Yang, Liang, Chang, 2019. Fabrication and characterization of the novel shape-stabilized composite PCMs of Na_2CO_3-K_2CO_3/MgO/glass. Sol. Energy 189, 228–234.

Yunxiu, Ren, Chao, Xu, Mengdi, Yuan, Feng, Ye, Xing, Ju, Xiaoze, Du, 2018. $Ca(NO_3)_2$-$NaNO_3$/expanded graphite composite as a novel shape-stable phase change material for mid- to high-temperature thermal energy storage. Energy Convers. Manage. 163, 50–58.

Zhiwei, Ge, Feng, Ye, Hui, Cao, Guanghui, Leng, Yue, Qin, Yulong, Ding, 2014. Carbonate-salt-based composite materials for medium-and high-temperature thermal energy storage. Particuology 15, 77–81.

Zhu, Jiang, Feng, Jiang, Chuan, Li, Guanghui, Leng, Xuemin, Zhao, Yunren, Li, Tongtong, Zhang, Guizhi, Xu, Yi, Jin, Cenyu, Yang, Yulong, Ding, 2019a. A form stable composite phase change material for thermal energy storage applications over 700 °c. Appl. Sci. 9, 814.

Zhu, Jiang, Guanghui, Leng, Feng, Ye, Zhiwei, Ge, Chuanping, Liu, Li, Wang, Yun, Huang, Yulong, Ding, 2015. Form-stable $LiNO_3$-$NaNO_3$-KNO_3-$Ca(NO_3)_2$/calcium silicate composite phase change material (PCM) for mid-low temperature thermal energy storage. Energy Convers. Manage. 106, 165–172.

Zhuo, Li, Zhi-Gen, Wu, 2016. Development of medium-temperature composite phase change material with high thermal stability and conductivity. Sol. Energy Mater. Sol. Cells 155, 341–347.